

Theory of the lattice Boltzmann method: discrete effects due to advection

Pierre Lallemand^a, François Dubois^{bc} and Li-Shi Luo^{ad}

^a *Beijing Computational Science Research Center, Haidian District, Beijing 100094, China.*

^b *Laboratoire de Mathématiques d'Orsay, Faculté des Sciences d'Orsay,
Université Paris-Saclay, France.*

^c *Conservatoire National des Arts et Métiers, LMSSC laboratory, Paris, France.*

^d *Department of Mathematics & Statistics, Old Dominion University, Norfolk, VA 23529, USA*

27 August 2022 *

Keywords: Lattice Boltzmann equation, Taylor expansion method, quartic parameters

PACS numbers: 02.70.Ns, 05.20.Dd, 47.11.+j.

Abstract

Lattice Boltzmann models are briefly introduced together with references to methods used to predict their ability for simulations of systems described by partial differential equations that are first order in time and low order in space derivatives. Several previous works have been devoted to analyzing the accuracy of these models with special emphasis on deviations from pure Newtonian viscous behaviour, related to higher order space derivatives of even order. The present contribution concentrates on possible inaccuracies of the advection behaviour linked to space derivatives of odd order. Detailed properties of advection-diffusion and athermal fluids are presented for two-dimensional situations allowing to propose situations that are accurate to third order in space derivatives. Simulations of the advection of a gaussian dot or vortex are presented. Similar results are discussed in appendices for three-dimensional advection-diffusion.

* A preliminary version of this contribution was presented by Pierre Lallemand at the International Conference for Mesoscopic Methods in Engineering and Science, Hambourg (Germany), 18-22 July 2016.

1) Introduction

Lattice Boltzmann models have been developed over almost three decades [7] based on microscopic physical models [9] and practices of numerical methods to solve PDE's [4]. The physical base is the notion of particles undergoing successive phases of free travel and collisions. Every function of the microscopic properties that is conserved in collisions will correspond to a macroscopic quantity that varies slowly in space and time and thus can be useful for computer simulations. The kinetic theory of gases has developed relationships between elementary motions and collisions of particles and partial differential equations describing the behavior of the relevant macroscopic quantities. It gives guidance to setting-up simplified models that may lead to useful numerical tools.

Computational fluid dynamics aims to predict the behavior of these quantities. It usually limits the description to a number of locations in space and at a number of times. Here we choose $t = n\delta t$, $\mathbf{r} := (i\hat{\mathbf{e}}_1 + j\hat{\mathbf{e}}_2)\delta r$ for 2-D problems and $\mathbf{r} := (i\hat{\mathbf{e}}_1 + j\hat{\mathbf{e}}_2 + l\hat{\mathbf{e}}_3)\delta r$ for 3-D problems, which are the “nodes” where the state of the fluid is defined, and $(\hat{\mathbf{e}}_1, \hat{\mathbf{e}}_2, \hat{\mathbf{e}}_3)$ are unit vectors for the spatial mesh. For simplicity further detailed expressions will be written for the 2-D case and some results will be given for 3-D cases.

In the basic Lattice Boltzmann Model (LBM), particles move synchronously between the various nodes, usually going to close neighbors in one time step. This allows to define a set of N elementary velocities of amplitude of the order of $\delta r/\delta t$, $\{c_p | p = 0, 1, \dots, N-1\}$, of Cartesian components (c_{px}, c_{py}) . At time n , the system is fully described by a set of $N \times M$ distribution functions $f_p(i, j, n)$ or by a point X in phase space $\Phi \in \mathbb{R}^{N \times M}$ for M active nodes. The dynamics is inspired from the Boltzmann equation. It consists in two steps:

(i) Local collision: $f_p(i, j, n) \mapsto f_p^*(i, j, n)$

(ii) Propagation to neighboring nodes:

$$f_p(i + c_{px}, j + c_{py}, n + 1) = f_p^*(i, j, n)$$

or from neighboring nodes:

$$f_p(i, j, n + 1) = f_p^*(i - c_{px}, j - c_{py}, n).$$

In the following, we define various Lattice Boltzmann models (Section 2), then explain the algorithm of generating the equivalent equations (Section 3), and the stability analysis in the linear case (Section 4). Then we present analytic results from the linear analysis (Section 5), including athermal fluid is simulated with the D2Q9 and the D2Q13 schemes. We study the distortion of a Gaussian dot or vortex in Section 6. Some technical precisions are presented in the appendices.

2) A brief description of the lattice Boltzmann equation

The lattice Boltzmann equation (LBE) evolves on a d dimensional lattice $\delta r \mathbb{Z}_d$ with lattice spacing δr and is fully defined by two ingredients: a set of discrete velocities $\mathbb{V} := \{\mathbf{c}_p\}$ and a collision model. Since the LBE is designed to simulate low-Mach-number flows, the discrete velocities \mathbb{V} is symmetric, that is, $-\mathbb{V} = \mathbb{V}$, or,

$$\forall \mathbf{c}_p \in \mathbb{V}, \quad \mathbf{c}_{\bar{p}} := -\mathbf{c}_p \in \mathbb{V},$$

thus, $\sum_p \mathbf{c}_p = \mathbf{0}$. Corresponding to each discrete velocity \mathbf{c}_p , there is a distribution function $f_p(\mathbf{r}_j, t_n)$ at every lattice point \mathbf{r}_j and each discrete time $t_n := n\delta t$, where $n \in \mathbb{N}_0 := \{0, 1, 2, \dots\}$ and δt is the time step size. In this setting, the unit of the velocity is $c := \delta r / \delta t$. The discrete velocity set \mathbb{V} , the set of nodes $\delta r \mathbb{Z}_d$, and the discrete time step size are tied together as follows :

$$\forall \mathbf{c}_p \in \mathbb{V} \text{ and } \mathbf{r}_j \in \delta r \mathbb{Z}_d, \quad \mathbf{r}_j + \mathbf{c}_p \delta t \in \delta r \mathbb{Z}_d.$$

The evolution of the lattice Boltzmann equation consists of two steps: (a) a local collision model

$$f_p(\mathbf{r}_j, n) \mapsto f_p^*(\mathbf{r}_j, n),$$

where $f_p(\mathbf{r}_j, n)$ and $f_p^*(\mathbf{r}_j, n)$ are the pre-collision and the post-collision states at the lattice node \mathbf{r}_j and the time t_n , respectively; and (b) propagation (or advection) from one lattice node \mathbf{r}_j to another $\mathbf{r}_j + \mathbf{c}_p \delta t$ in one time step according to discrete velocities \mathbf{c}_p :

$$f_p(\mathbf{r}_j + \mathbf{c}_p \delta t, n + 1) = f_p^*(\mathbf{r}_j, n).$$

A LBM model is fully defined by two pieces of information: the set of elementary velocities and the rules that govern the collision step. As one usually aims to simulate fluid flows, it is highly suggested to use a set of elementary velocities as isotropic as possible. This means using orthogonal coordinates and for each possible velocity amplitude, sets obtained by symmetry and permutation of the axis.

Note that one can also use 6 velocities based on the hexagon, but this cannot be extended to 3-D cases.

We will adopt the notation of DdQq for a model in d -dimensional space with q velocities. In this work we shall mostly focus on the lattice Boltzmann (LB) models in space of two dimensions (2D). The most often used thirteen discrete velocities in 2D are listed in Table 1. We note that these discrete velocities conform with the Cartesian square lattice in 2D. However, it is possible also to use a triangular lattice in 2D [5]. Obviously, the Cartesian lattice in 2D can be easily extended to 3D.

Number	$ \mathbf{c}_p/c ^2$	\mathbf{c}_p/c
1	0	(0, 0)
4	1	(1, 0), (0, 1), (-1, 0), (0, -1)
4	2	(1, 1), (-1, 1), (-1, -1), (1, -1)
4	4	(2, 0), (0, 2), (-2, 0), (0, -2)

Table 1: The first 13 discrete velocities used in the various lattice Boltzmann models.

We consider simple *local* collision model that gives prevalence to the notions of “conservation” and symmetry, two equivalence concepts according to Nöther. In this work we will use the linear relaxation model proposed by d’Humières [7], in which the collision process is modeled by the linear relaxations of the velocity moments $\{m_p\}$ of the distribution functions $\{f_p\}$.

Given a set $\{\mathbf{c}_p | p = 0, 1, \dots, (q-1)\}$ of q discrete velocities, there always exists a $q \times q$ invertible matrix \mathbf{M} such that

$$(1) \quad \mathbf{m} = \mathbf{M}\mathbf{f}, \quad \mathbf{f} = \mathbf{M}^{-1}\mathbf{m},$$

where \mathbf{f} and \mathbf{m} denote the vectors of q dimensions of the distribution functions $\{f_p\}$ and the moments $\{m_p\}$, respectively, *i.e.*,

$$\begin{aligned} \mathbf{f} &:= (f_0, f_1, \dots, f_{q-1})^\dagger, \\ \mathbf{m} &:= (m_0, m_1, \dots, m_{q-1})^\dagger, \end{aligned}$$

where \dagger denotes transpose. It is convenient to use orthogonal polynomials on the discrete velocity set \mathbb{V} so that the relaxation processes of moments are independent to each other. The orthogonal polynomials with respect to a weight of unity for the models up to thirteen velocities in 2D are given in Table 2. Denote the polynomials in Table 2 by $P_q(\mathbf{c}_p)$, then the transformation matrix can be constructed with its matrix elements given by $P_q(\mathbf{c}_p)$, *i.e.*, $\mathbf{M}_{pq} = P_q(\mathbf{c}_p)$.

in the use at each node of a linear transformation of the set of distribution functions f_p to moments based on polynomials of the elementary velocities components of increasing order chosen as isotropic as possible. It is also convenient to orthogonalize the moments of the same symmetry. This allows to define a “moment matrix” M that relates the distributions f_p and the moments m_p by $m = Mf$. (Note that M must be invertible.) We use for a 2-D model with N velocities the nomenclature D2QN. The polynomials used to generate M (by replacing (x, y) by (c_{px}, c_{py}) for each elementary velocity) are:

model	Orthogonal Polynomials on \mathbb{V} , $r := \sqrt{x^2 + y^2}$
D2Q1	1
D2Q5	$1, x, y, -4 + 5r^2, x^2 - y^2$
D2Q9	$1, x, y, -4 + 3r^2, x^2 - y^2, xy,$ $-(5 - 3r^2)x, -(5 - 3r^2)y, 4 - \frac{3}{2}(7 + 3r^2)r^2$
D2Q13	$1, x, y, -28 + 13r^2, x^2 - y^2, xy,$ $-(3 - r^2)x, -(3 - r^2)y,$ $\frac{1}{12}(202 - 189r^2 + 35r^4)x, \frac{1}{12}(202 - 189r^2 + 35r^4)y,$ $-\frac{1}{2}(280 - 361r^2 + 154r^4), -\frac{1}{12}(65 - 17r^2)(x^2 - y^2),$ $-\frac{1}{24}(288 - 1162r^2 + 819r^4 - 137r^6)$

Table 2: The orthogonal polynomials for the moments in D2Q q lattice Boltzmann models, with $q = 1, 5, 9$ and 13. For 3-D cases, see Appendix-2

Similar expressions can be obtained for 3-D cases (see Appendix 2). The successive moments can be interpreted as density ρ , components of momentum $\{j_x, j_y\}$, kinetic energy (E), components of the stress tensor, components of heat flux, and so on.

Depending on which situation is to be simulated, we shall consider that in situations of dimensionality d , there are 1, $d + 1$ or $d + 2$ moments conserved in collisions. Either $\{\rho\}$,

or $\{\rho, j_x, j_y\}$ or $\{\rho, j_x, j_y, E\}$ allow to simulate respectively advection–diffusion, athermal Navier–Stokes, Navier–Stokes problems for $d = 2$. The other moments (non-conserved moments) evolve with simple linear relaxation:

$$(2) \quad m_p^* = m_p + s_p(m_p^{eq} - m_p)$$

where s_p is a relaxation rate and m_p^{eq} the equilibrium value of the moment m_p . We consider that m_p^{eq} is a function of the local conserved quantities and that the relaxation rates are given values.

Numerous papers [7, 8, 9] and practices of numeric have analyzed the behavior of the model described above in situations where conserved quantities vary slowly in space and time (on time or spatial scales large compared to the elementary units δt or δr .) A popular approach is to follow the kinetic theory approach with the Chapman–Enskog expansion. An alternative way proposed by one of us performs a Taylor expansion assuming smooth behavior of the conserved quantities.

The method involves an expansion of the non-conserved moments in powers of the time increment δt (considered as a small quantity)

$$m = m^{(0)} + \delta t m^{(1)} + \delta t^2 m^{(2)} + \dots$$

and to get iteratively the terms $m^{(l)}$. One gets expressions that involve space derivatives of the conserved moments of increasing order together with time derivatives. At each step of the process higher order time derivatives are eliminated by using the results of the previous step.

This leads to equivalent PDE’s relating the conserved quantities that are first order in time derivatives and of desired order in space derivatives (somewhat like in the hierarchy Euler, Navier–Stokes, Burnett, super–Burnett, *etc*). A careful analysis of the iterative process allows to state whether adding more elementary velocities improves the accuracy of the results already available. Note however that these approaches (Chapman–Enskog, Taylor expansion, *etc*.) don’t give all the necessary information concerning numerical stability of the method. Useful results, although not complete, are provided by the study of the dispersion equation for plane waves summarized in appendix 1. The equivalent equations method allows to obtain expressions for higher order terms and thus to discuss resulting inaccuracies and in some cases ways to improve the models. Some results are presented below.

3) Generation of equivalent equations

Here we describe the principle of the generation of equivalent equations.

• Ingredients

To completely define the LBE process, we need the following ingredients :

-List of elementary velocities, here $\{c_{ix}, c_{iy}\}$. (to simplify writing we take units such that c_i is of the order of 1, and thus will have just one small parameter to deal with when making expansions. This is sometimes called the “acoustic scaling”.)

- Matrix of moments M (of dimension $n \times n$), and M^{-1} its inverse.
- List of moments conserved in collision W (of dimension n_c equal either to 1 or to 3)
- List of equilibrium values of the non-conserved moments M^{eq} ($n - n_c$), which depend on the local values of the conserved quantities W .
- List of relaxation rates for the non-conserved moments S ($n - n_c$).
- Time evolution of the LBE process written in f space as n equations :

$$(3) \quad f_j(t + \Delta t, r) = f_j^*(t, r - c_j \Delta t)$$

where the superscript $*$ indicates a “post-collision” quantity and Δt is the small parameter for expansions.

The collision step is performed in moment-space, whereas the propagation step is performed in f -space.

• Iterative process

We assume “smoothly varying” behaviour for all quantities to be dealt with. Then we can expand the relation (3) at various orders of accuracy relative to the small parameter Δt . At order zero, we find that the pre-collision distribution f is close to the post-collision particle distribution f^* :

$$f^* = f + O(\Delta t).$$

When we re-write this relation in terms of the moments m , we deduce from the previous relation and the basic iteration of the lattice Boltzmann scheme

$$(4) \quad m_k^* = m_k + s_k (m_k^{eq} - m_k)$$

the fact that both m and m^* are close to the equilibrium

$$(5) \quad m = m^{eq} + O(\Delta t), \quad m^* = m^{eq} + O(\Delta t).$$

• Order one

After this first step, we expand the relation (3) at the order one, transform the particles into moments and replace the moments in the first order terms by their equilibrium values. We obtain by this way:

$$(6) \quad m_k + \Delta t \frac{\partial m_k^{eq}}{\partial t} + O(\Delta t^2) = m_k^* - \Delta t \sum_{j\ell\alpha} M_{kj} c_j^\alpha M_{j\ell}^{-1} \frac{\partial m_\ell^{eq}}{\partial x^\alpha} + O(\Delta t^2).$$

For the moments that are equilibrium, *id est* $m_k \equiv m_k^*$, the relation (6) gives immediatly the equivalent partial differential equations at order one:

$$(7) \quad \frac{\partial m_k^{eq}}{\partial t} + \sum_{\ell\alpha} \left(\sum_j M_{kj} c_j^\alpha M_{j\ell}^{-1} \right) \frac{\partial m_\ell^{eq}}{\partial x^\alpha} = O(\Delta t).$$

Moreover, for the moments m_k that are not at equilibrium, we extract the difference $m_k - m_k^*$ from the relations (4) and (6). Then a first order expansion for these non-conserved moments emerge:

$$m_k = m_k^{eq} - \frac{\Delta t}{s_k} \left(\frac{\partial m_k^{eq}}{\partial t} + \sum_{\ell\alpha} \left(\sum_j M_{kj} c_j^\alpha M_{j\ell}^{-1} \right) \frac{\partial m_\ell^{eq}}{\partial x^\alpha} \right) + O(\Delta t^2).$$

It is then usefull to explicit the nonconserved moments afer relaxation, using (4) and the previous relation:

$$(8) \quad m_\ell^* = m_\ell^{\text{eq}} + \left(1 - \frac{1}{s_\ell}\right) \Delta t \left(\frac{\partial m_\ell^{\text{eq}}}{\partial t} + \sum_{\ell\beta} \left(\sum_j M_{\ell j} c_j^\beta M_{jp}^{-1} \right) \frac{\partial m_p^{\text{eq}}}{\partial x^\beta} \right) + O(\Delta t^2).$$

• **Expansion at order two and more**

The next step is to expand the relation (3) up to second order accuracy; due to (5), we can replace the moments m and m^* by their equilibrium values for the second order terms. We obtain in this way

$$(9) \quad \begin{cases} m_k + \Delta t \frac{\partial m_k}{\partial t} + \frac{\Delta t^2}{2} \frac{\partial^2 m_k^{\text{eq}}}{\partial t^2} = m_k^* - \Delta t \sum_{j\ell\alpha} M_{kj} c_j^\alpha M_{j\ell}^{-1} \frac{\partial m_\ell^*}{\partial x^\alpha} \\ \quad + \frac{\Delta t^2}{2} \sum_{j\ell\alpha\beta} M_{kj} c_j^\alpha c_j^\beta M_{j\ell}^{-1} \frac{\partial^2 m_\ell^{\text{eq}}}{\partial x^\alpha \partial x^\beta} + O(\Delta t^3). \end{cases}$$

In the expansion (9), there are three terms of order 2: $\frac{\partial^2 m_k^{\text{eq}}}{\partial t^2}$ in the left hand side, the term $\sum_{j\ell\alpha\beta} M_{kj} c_j^\alpha c_j^\beta M_{j\ell}^{-1} \frac{\partial^2 m_\ell^{\text{eq}}}{\partial x^\alpha \partial x^\beta}$ in the right hand side and the term induced by the expansion (8) inside the first order term $\frac{\partial m_\ell^*}{\partial x^\alpha}$ in the left hand side. After taking a careful attention of all these terms, we obtain the partial equivalent equations at order 2. For the end of the computation at second order, we refer to our original contribution [2]. For the extension at fourth order in a general nonlinear approach, we refer to [3]. The extention to linearised schemes at fourth order accuracy has been proposed in [4]. The algorithm has been simplified in [1]. In this contribution, we have used this last version, also called ‘‘Berlin algorithm’’.

The basic development is made in terms of moments :

$$(10) \quad m_i = m_i^0 + m_i^1 \Delta t + m_i^2 \Delta t^2 + \dots$$

and we go back and forth between f-space and m-space with matrices M or M^{-1} as necessary. At order 0, m_i^0 is the set of the n_c conserved moments + equilibrium values of the $n - n_c$ other moments.

We expand Eq. 3 in powers of Δt and collect the various powers of Δt , The ‘‘propagation’’ on the right hand side of Eq. 3 increases the order in Δt by one unit, so one gets expressions of the type

$$(11) \quad \sum_p \partial_t^p m_i^{q-p} = \sum A \partial^p m_i^{q-1-p}$$

where A is an operator expressed in powers of $M^{-1}PM$ where P is linked to the velocity set. This allows to get iteratively the values of the non-conserved moments in terms of space and time derivatives of the conserved quantities W . There are however unwanted time derivatives of order larger than 1. They are eliminated iteratively using the results previously derived. The complexity of the expressions increases very fast with the order of the iterations, so some

care is needed to estimate which contributions can be safely discarded. The net result is either 1 or 3 partial differential equations of the W quantities that are first order in time and high order in space and so can be directly compared to classic PDE's (Euler, Navier-Stokes, etc...).

4) Linear Analysis of Lattice Boltzmann Models in 2D

A practical approach to the study of stability is described below. Several important features of the ability of a LBM model to simulate physical flows can be obtained for specialized situations that provide a lot of useful information. Consider a domain with $\{N_x, N_y\}$ active nodes and periodic boundary conditions. One looks for solutions of the form

$$(12) \quad m_p(i, j, n) = A_p a_p^i b_p^j z^n$$

So we take an initial condition periodic in space:

$$(13) \quad m_p(i, j, 0) = m_{p0} \phi_{px}^i \phi_{py}^j + M_{p0}$$

using phase factors $\phi_{px} = \exp(ik_x c_{px})$ and $\phi_{py} = \exp(ik_y c_{py})$. $\{k_x, k_y\}$ can be interpreted as components of the wave vector and M_{p0} is linked to a uniform field (say uniform density and constant background velocity, a situation allowing to test Galilean invariance of the models). One can compute the moments m_{p1} at time $n = 1$. Assuming that the initial amplitudes m_{p0} are small, one linearizes the new values with respect to m_{p0} . If the components of the wave vector are compatible with the periodicity conditions, $-k_x N_x$ and $k_y N_y$ are multiple of 2π – then the expressions for the new values are the same at all points (m_{p1} within a simple phase factor). The problem thus simplifies to a $q \times q$ problem. One gets

$$(14) \quad m_{p1} = E m_{p0} = z m_{p0}$$

with a matrix \mathbf{G} defined by q equations in “ f_{space} ”:

$$(15) \quad G_p = (I + M^{-1} C M) \phi_{px} \phi_{py}$$

and the corresponding one in “ m_{space} ”, $E = M G M^{-1}$. C corresponds to the collision step and can be obtained from Eq. (2). Under such periodic conditions, analysis can be made at a single node, and so one just needs to consider q -dimensional vectors

$$\Phi = \{f_0, \dots, f_{q-1}\}$$

as elements of phase space, together with the scalar product defined as

$$(16) \quad \langle \Phi^1 | \Phi^2 \rangle = \sum_{p=0}^{q-1} f_p^1 f_p^2$$

Note that when this is applied to the moments m_p , sums of products of small integers are involved and so there may be accidental degeneracies. It may therefore be quite useful to

determine the rank of the parts of the moment matrix M corresponding to moments of the same orders.

The determination of the eigenvalues and eigenfunctions of E can be done with the dispersion equation formalism. For particular values of the wave vector, this can be done analytically. In particular for $k_x = k_y = 0$ one gets $z_p = 1 - s_p$ indicating that $0 \leq s_p \leq 2$ for stability. For small values of the wave vector, one can solve the dispersion equation by successive approximations for the roots z_l close to 1 then compute $\gamma_l = \log(z_l)$ that will be compared to the predictions of the standard PDE's. When numerical values of all parameters present in E are given, one can use fast linear algebra packages (for instance in LAPACK) for several values of the components of the wave vector. Any situation leading to an eigenvalue z_l with modulus greater than 1 is numerically unstable and therefore not suitable for simulations. It is found that this usually occurs for "large" values of k_x or k_y (say between 1 and π) so developments in k_i near $k = 0$ are often not able to predict the corresponding instability.

5) Analytic results from the linear analysis

• D2Q5 model for advection-diffusion equation in 2D

It has been known for a long time that a 5 velocity (D2Q5) model can be used to simulate advection-diffusion in 2-D.

$$(17) \quad \partial_t \rho + \mathbf{V} \cdot \nabla \rho - \kappa \Delta \rho = 0.$$

However it is found that the effective diffusivity κ varies as the square of the advective velocity. This is not satisfactory so one can use D2Q9 with adequate expressions for the equilibrium of the non-conserved moments.

We shall use the following Table 3, where V_x and V_y are the x and y components of the advective velocity \mathbf{V} , respectively, and u and a parameters for optimization.

Moment	Parity	Rate	Equilibrium
ρ	+	0	ρ
j_x	−	s_1	ρV_x
j_y	−	s_1	ρV_y
E	+	s_3	$\rho (\alpha + 3V^2)$
p_{xx}	+	s_4	$\rho (V_x^2 - V_y^2)$
p_{xy}	+	s_4	$\rho V_x V_y$
q_x	−	s_6	$d_1 \rho V_x$
q_y	−	s_6	$d_1 \rho V_y$
ϖ	+	s_8	$\rho (\beta + a V^2)$

Table 3: D2Q9 equilibrium moments for advection-diffusion, including two parameters, u and a , for further optimization. $V^2 := V_x^2 + V_y^2$.

The choice of relaxation rates and expressions in terms of velocity was made in accordance to the symmetry of the set of elementary velocities (the parity is indicated in the second column to be used for the particular two-relaxation times (TRT) models).

Applying the Taylor expansion method in the linear case with the so-called “Berlin algorithm” [1] to third order in space derivatives and neglecting non linear terms in density, one gets one equivalent equation for the density:

$$(18) \quad \partial_t \rho + \mathbf{V} \cdot \nabla \rho - \kappa \Delta \rho = O(\nabla^3 \rho),$$

where the diffusivity κ is independent of velocity:

$$(19) \quad \kappa = \frac{\alpha + 4}{6} \left(\frac{1}{s_1} - \frac{1}{2} \right).$$

The next order

$$(20) \quad O(\nabla^3) = \sum_{\alpha\beta\gamma} H_{\alpha\beta\gamma}(\mathbf{V}) \partial_{\alpha\beta\gamma}^3 \rho, \quad \alpha, \beta, \gamma \in \{x, y\},$$

leads to corrections to advection and thus corresponds to the aim of the present report.

Considering a plane wave $\rho(\mathbf{r}, t) = \exp(\gamma t) \exp(i\mathbf{k} \cdot \mathbf{r})$ and taking only contributions linear in velocity in Eq. (18), the phase velocity is

$$(21) \quad \mathbf{V} \cdot \mathbf{k} [1 + A(\mathbf{k}, \hat{\mathbf{V}})].$$

From now on, we refer to $A(\mathbf{k}, \hat{\mathbf{V}})$ as the “anomalous advection” and we try and minimize its magnitude.

This correction factor $A(\mathbf{k}, \hat{\mathbf{V}})$ is a complicated function depending on the orientations (with respect to the computational grid) of both the velocity \mathbf{V} and the wave-vector \mathbf{k} . However it becomes independent of orientations when

$$(22) \quad d_1 = -1 \quad \text{or} \quad \sigma_1 \sigma_4 = \frac{1}{12},$$

where we use the Hénon parameters [6] defined by $\sigma_i = \frac{1}{s_i} - \frac{1}{2}$. Note that the condition for isotropy of the shear viscosity of the standard D2Q9 model leads also to the equivalent value for the parameter $c_1 = -1$.

When $d_1 = -1$, the correction to advection becomes:

$$(23) \quad A_1 = \frac{1}{24} [2 + \alpha + 4(\alpha\sigma_3 - 2\sigma_4)\sigma_1 + 8(4 + \alpha)\sigma_1^2],$$

and when $\sigma_1 \sigma_4 = \frac{1}{12}$, it reduces to

$$(24) \quad A_2 = \frac{1}{72} [7 - d_1 + 3\alpha + 12\sigma_1\sigma_3(1 - \alpha + d_1) - 24\sigma_1^2(4 + \alpha)].$$

Both expressions can be put to 0 by suitable choice of the parameters σ_i provided stability of the process is satisfied.

We mention that the next order in the equivalent equation Eq. (18) gives rise to a correction to the viscous term, allowing to define the “hyper-diffusivity”. This has been studied for

$V_x = V_y = 0$ in ref. [4]. The results presented here for the D2Q9 model can be extended to 3-dimensional situations. The simplest model is based on D3Q7 with elementary velocities $\{0, 0, 0\}$, $\{1, 0, 0\}$, $\{-1, 0, 0\}$, $\{0, 1, 0\}$, $\{0, -1, 0\}$, $\{0, 0, 1\}$, $\{0, 0, -1\}$. However the effective diffusivity is velocity-dependent. Therefore models based on D3Q15 or D3Q19 have been proposed. The basic properties of these models for advection-diffusion and the tuning of parameters to get rid of anomalous advection are summarized in Appendix 2.

• Athermal fluid simulated with D2Q9

We start with the common D2Q9 model with 3 conservations defined by the Table 4. Applying the Taylor expansion analysis up to third order in space derivatives leads to a hierarchy of equivalent equations for ρ, j_x, j_y analogous to Equ. 18. As we consider only the linear behavior of the three conserved quantities it is convenient to express the results in terms of matrices for the successive orders in space derivatives (shown later as N_0, N_1, N_2 and N_3).

Moment	Parity	Rate	Equilibrium
ρ	+	0	ρ
j_x	−	0	j_x
j_y	−	0	j_y
E	+	s_3	$\rho \left(\alpha + 3 \frac{j_x^2 + j_y^2}{\rho} \right)$
XX	+	s_4	$\frac{j_x^2 - j_y^2}{\rho}$
XY	+	s_4	$\frac{j_x j_y}{\rho}$
q_x	−	s_6	$-\dot{j}_x$
q_y	−	s_6	$-\dot{j}_y$
ϖ	+	s_8	$\rho \left(\beta - 3 \frac{j_x^2 + j_y^2}{\rho} \right)$

Table 4: Equilibrium values of the D2Q9 moments for fluid equations.

The first order, which aims to match Euler's equations, is

$$(25) \quad \mathbf{M}_0 + \mathbf{M}_1 = \begin{pmatrix} \frac{\partial_t}{6} & \frac{\partial_x}{6} & \frac{\partial_y}{6} \\ \frac{(\alpha+4)}{6} \partial_x - V_x \mathbf{V} \cdot \nabla & \partial_t + \mathbf{V} \cdot \nabla + V_x \partial_x & V_x \partial_y \\ \frac{(\alpha+4)}{6} \partial_y - V_y \mathbf{V} \cdot \nabla & V_y \partial_x & \partial_t + \mathbf{V} \cdot \nabla + V_y \partial_y \end{pmatrix}$$

higher orders \mathbf{M}_l are cumbersome and not given here.

Starting from initial conditions

$$(26a) \quad \rho(x, y, t) = 1 + \rho_0 \exp(\omega t) \cos(\mathbf{k} \cdot \mathbf{r}),$$

$$(26b) \quad \mathbf{J}(x, y, t) = \mathbf{V} + \mathbf{J}_0 \exp(\omega t) \cos(\mathbf{k} \cdot \mathbf{r}),$$

we apply the matrices \mathbf{M}_l and show results just for the particular case where the mean velocity is orthogonal to the wave vector. In addition we apply a rotation of the axis such that the wave vector is along the axis Ox :

$$(27) \quad N_0 = \begin{pmatrix} \omega & 0 & 0 \\ 0 & \omega & 0 \\ 0 & 0 & \omega \end{pmatrix},$$

$$(28) \quad N_1 = \begin{pmatrix} 0 & 1 & 0 \\ \frac{\alpha+4}{6} & 0 & 0 \\ 0 & V & 0 \end{pmatrix} k,$$

$$(29) \quad N_2 = \begin{pmatrix} 0 & 0 & 0 \\ 0 & (\alpha\sigma_3 - 2\sigma_4)(1 - 3V^2) & 0 \\ (\alpha + 4)\sigma_4 V & 0 & -2\sigma_4 \end{pmatrix} \frac{k^2}{6}.$$

Note that Navier-Stokes equations can be expressed just with these three matrices but without the off-diagonal terms $N_1(3, 2)$ and $N_2(3, 1)$ and the velocity in $N_2(2, 2)$.

At order 3, taking the usual values of the parameters $\alpha = -2$ and $\beta = 1$ in order to simplify the expressions, one gets:

$$(30) \quad N_3 = \begin{pmatrix} 0 & -\frac{1}{18} & 0 \\ h_0 + h_1 V^2 & g_1 f_1(\theta) & h_3 V - g_3 V f_2(\theta) \\ g_2 V^2 f_1(\theta) & h_4 V - g_2 V^2 f_1(\theta) & g_2 V f_1(\theta) \end{pmatrix} k^3$$

with

$$(31) \quad \begin{cases} f_1(\theta) = \sin 4\theta, \quad f_2(\theta) = \sin^2 2\theta, \\ h_0 = \frac{1 - 3(\sigma_3^2 + \sigma_4^2)}{27}, \\ h_1 = \frac{(\sigma_3 + 3\sigma_4 - 2\sigma_6)(\sigma_3 - \sigma_4)}{6}, \quad h_3 = \frac{(\sigma_4 - 2\sigma_6)(\sigma_3 - \sigma_4)}{3}, \\ g_1 = \frac{1 - 6\sigma_6(\sigma_3 + \sigma_4)}{24}, \quad g_2 = \frac{1 - 12\sigma_4\sigma_6}{24}, \quad g_3 = \frac{1 + 12\sigma_6(\sigma_3 - 2\sigma_4)}{24}, \\ h_4 = \frac{1 + 6\sigma_4(\sigma_3 + \sigma_4 - 2\sigma_6)}{18} \end{cases}$$

where the relaxation rates appear as

$$(32) \quad \sigma_3 = \frac{1}{s_E} - \frac{1}{2}$$

for the energy mode,

$$(33) \quad \sigma_4 = \frac{1}{s_{XX}} - \frac{1}{2}$$

for components of the stress tensor, and

$$(34) \quad \sigma_6 = \frac{1}{s_{qx}} - \frac{1}{2}$$

for the components of the heat flux. This third order matrix becomes independent of the angle θ for

$$(35) \quad \sigma_3 = \sigma_4 \quad \text{and} \quad \sigma_4 \sigma_6 = \frac{1}{12}$$

leading to

$$(36) \quad N_3^{\text{isotropic}} = \begin{pmatrix} 0 & 3(\alpha - 2) & 0 \\ (\alpha + 4)(\alpha - 2)(6\sigma_4^2 - 1) & 0 & 0 \\ 0 & 6(\alpha(12\sigma_4^2 - 1) - 2) & 0 \end{pmatrix} \frac{k^3}{216}$$

One can then obtain the complex relaxation rate of the waves.

Transverse wave and V perpendicular to k

At order 1 in k , the phase velocity is 0.

At order 2 in k , the attenuation is $-\sigma_4/3k^2$, we recover the usual shear dynamic viscosity

$$\nu_0 = \frac{1}{3}\sigma_4$$

At order 3 in k , one gets a phase velocity

$$(37) \quad v_\varphi = \frac{1}{24}V(1 - 12\sigma_4\sigma_6)\sin 4\theta.$$

Transverse wave and V parallel to k

At order 1 in k , the phase velocity is V .

At order 2 in k , the attenuation corresponds to an effective shear viscosity

$$(38) \quad \nu_{\text{eff}} = \frac{1}{3}\sigma_4(1 - 3V^2) = \nu_0(1 - 3V^2).$$

At order 3 in k , the phase velocity is modified (at first order in V) by

$$(39) \quad \frac{1}{24}[16\sigma_4(\sigma_4 - \sigma_6) + (1 - 12\sigma_4\sigma_6)f_2(\theta)]V.$$

Similarly expressions are readily obtained for acoustic waves when $V = 0$ [4]; cancellation of the corresponding expression occurs for the particular case $\nu_{\text{eff}} = 1/\sqrt{108}$, which may be referred to as a “quartic condition” which can be seen as the cancellation of the “hyper-viscosity”.

• Athermal fluid simulated with D2Q13

Similar expressions have been derived for the D2Q13 model[†] and we just give the results of the analysis of the waves, using for the relaxation rates

$$(40) \quad \sigma_4 = \frac{1}{s_{XX}} - \frac{1}{2}$$

for components of the stress tensor, and

$$(41) \quad \sigma_6 = \frac{1}{s_{qx}} - \frac{1}{2}$$

for the components of the heat flux, and

$$(42) \quad \sigma_8 = \frac{1}{s_{rx}} - \frac{1}{2}$$

for the components of the “next” heat flux.

Transverse wave and V perpendicular to k

At order 1 in k , the phase velocity is 0.

At order 2 in k , the effective shear viscosity is

$$(43) \quad \nu_{\text{eff}} = \frac{3 + c_1}{4} \sigma_4 \left[1 - \frac{12(7 + 6q)}{77(3 + c_1)} V^2 \right] = \nu_0 \left[1 - \frac{12(7 + 6q)}{77(3 + c_1)} V^2 \right]$$

showing that one can eliminate the velocity dependence of the effective shear viscosity for the particular value of the parameter $q = -7/6$.

At order 3 in k , there is an additional phase velocity

$$(44) \quad v_\varphi = \frac{\sigma_4(89772 \sigma_6 + 30888 \sigma_8) - 10055}{157080} V \sin 4\theta$$

Transverse wave and V parallel to k

At order 1 in k , the phase velocity is V .

At order 2 in k , the effective shear viscosity is

$$(45) \quad \nu_{eff} = \frac{3 + c_1}{4} \sigma_4 \left(1 - \frac{12}{77} \frac{7 + 6q}{3 + c_1} V^2 \right)$$

showing that the velocity dependence is the same as in the previous case.

At order 3 in k , the phase velocity is modified by

$$(46) \quad v_\varphi = \left[\sigma_4 \left(\frac{128 - 306c_1}{85} \sigma_6 + \frac{306c_1 + 182}{85} \sigma_8 \right) - \frac{31}{102} \right] V f_2(\theta) \\ + \left[\sigma_4 \left(-\frac{1 + c_1}{5} \sigma_6 + \frac{9c_1 - 1}{20} \sigma_8 \right) - \frac{5 + 3c_1}{48} + \frac{3 + c_1}{2} \sigma_4^2 \right] V.$$

[†]See Appendix 2 for details on the relaxation step

It is possible to remove the angular dependence by taking

$$(47) \quad \sigma_6 = \sigma_8 = \frac{1}{12\sigma_4}$$

which leads to an additional phase velocity

$$(48) \quad v_\varphi = \frac{3+c_1}{24} (12\sigma_4^2 - 1) V.$$

The special value $\sigma_4 = \frac{1}{\sqrt{12}}$ allows to get rid of the additional phase velocity.

In the general case of arbitrary orientations of the wave vector \mathbf{k} and of the advection speed V , expressions are quite complicated. Some information on the relative importance of the corrections to the advection are shown in Fig. 1. The advection term is computed numerically as

$$(49) \quad g(\mathbf{k}) = \mathbf{k} \cdot \mathbf{V} (1 + h k^2)$$

with h depending on the orientation of both \mathbf{k} and \mathbf{V} . It is represented in Fig. 1 as solid curve for D2Q13 and a dashed curve for D2Q9 for \mathbf{V} parallel to Ox and \mathbf{k} at angle θ .

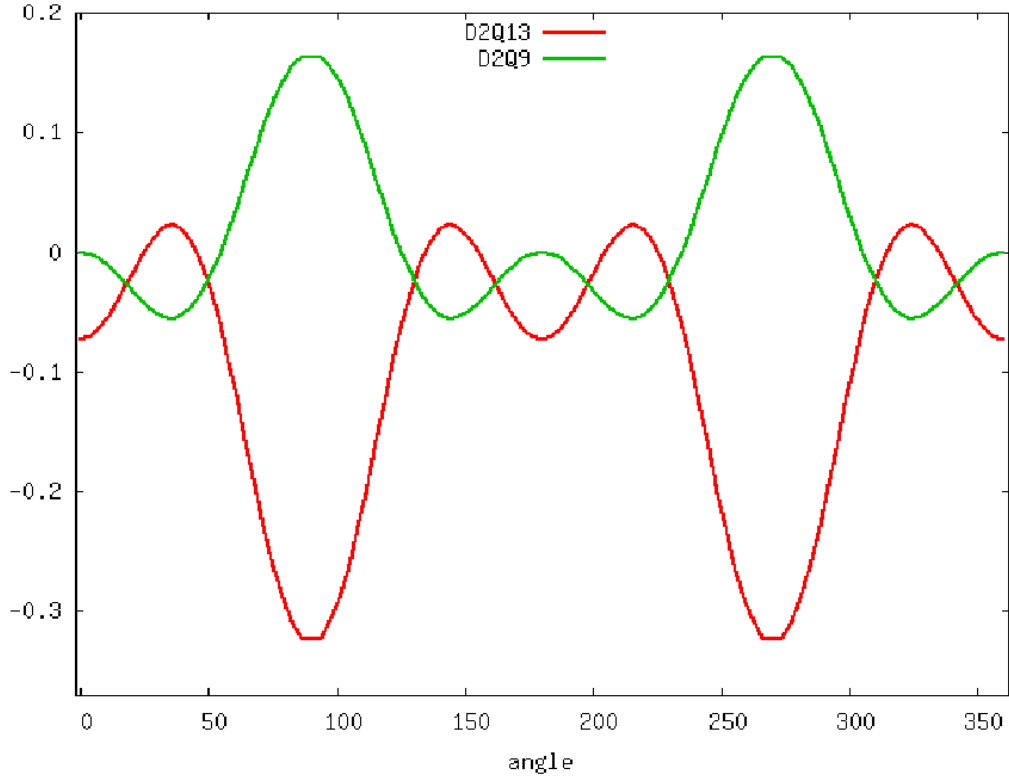


Figure 1: Advection factor for main velocity along Ox axis and wave vector vs angle θ . Dotted line in the absence of anomalous advection. Solid line contribution h for D2Q13, dashed line for D2Q9.

Some consequences of the correction to advection are presented below.

6) Distortion of a Gaussian initial conditions

Consider the following Gaussian initial condition

$$(50) \quad \Gamma(r, 0) = g_0 \exp \left[- \left(\frac{r}{r_0} \right)^2 \right],$$

centered at the origin $= (0, 0)$, where $r := \sqrt{x^2 + y^2}$ is the distance to the center. When the Gaussian initial condition $\Gamma(r, 0)$ is used as the initial density $\rho(r, 0)$ of the advection-diffusion equation or the initial stream function $\psi(r, 0)$ of the Navier-Stokes equation, the solution for both cases is

$$(51) \quad \Gamma(r, t) = g_0 \frac{r_0^2}{r_0^2 + 4\chi t} \exp \left[- \frac{(\mathbf{r} - \mathbf{V}t) \cdot (\mathbf{r} - \mathbf{V}t)}{r_0^2 + 4\chi t} \right]$$

in the presence of a uniform velocity $\mathbf{V} := (V_x, V_y)$ [10], where $\chi = \kappa$ for the advection-diffusion equation and $\chi = \nu$ for the Navier-Stokes equation.

The solution $\Gamma(r, t)$ is invariant under rotation.

The results of simulation are shown below for several cases.

$$(52) \quad \psi(r, 0) = g_0 \exp \left[- \left(\frac{r}{r_0} \right)^2 \right]$$

or the initial stream function $\psi(r, 0)$ for the Navier-Stokes (centered at the origin $\{0,0\}$ and r is the distance to the center), evolve as

$$(53) \quad \Gamma(r, t) = g_0 \frac{r_0^2}{r_0^2 + 4\kappa t} \exp \left[- \frac{(\mathbf{r} - \mathbf{V}t) \cdot (\mathbf{r} - \mathbf{V}t)}{r_0^2 + 4\kappa t} \right]$$

or

$$(54) \quad \psi(r, t) = g_0 \frac{r_0^2}{r_0^2 + 4\nu t} \exp \left[- \frac{(x - V_x t)^2 + (y - V_y t)^2}{r_0^2 + 4\nu t} \right]$$

in the presence of a uniform velocity $\mathbf{V} := (V_x, V_y)$ [10]. The computed field is invariant by rotation. The results of simulation are shown below for several cases.

Diffuse D2Q9

Fig. 2 shows the distribution of $\rho(x, y)$ for three different conditions. The computation is done on a square domain 101^2 with periodic boundary conditions. The main parameters are: $\kappa = 0.008$, $V_x = 0.10$, $V_y = 0$ and 3200 time steps. Initial radius is $r_0 = 5.0$ and initial locations are chosen so that final states do not overlap. The top feature is obtained with $q = -1$, the lower feature is obtained with $12\sigma_1\sigma_4 = 1$ and one can verify that the results are close to rotational invariance. The right feature satisfies neither of the isotropy conditions and it is clear that it is not rotationally invariant.

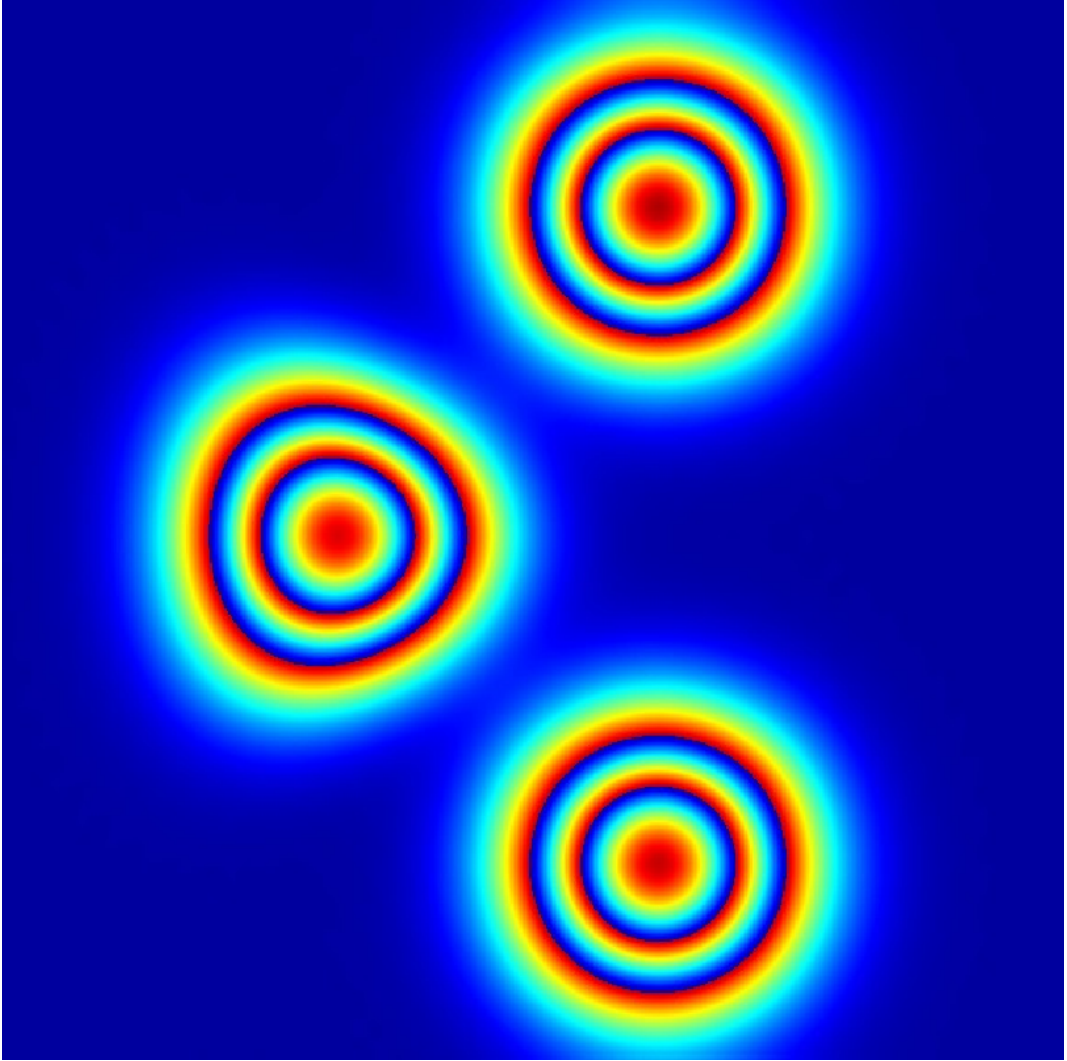


Figure 2: Advection of an initial Gaussian disturbance simulated with diffusive D2Q9 under conditions described in the text. Top and lower features are isotropic (respectively for $q = -1$ or $12\sigma_1\sigma_4 = 1$). The middle feature uses conditions that are not tuned for isotropy.

Navier–Stokes D2Q9

Simulation of the D2Q9 model have been performed in a 301^2 domain with periodic boundary conditions. The initial condition is uniform speed (indicated in the caption), the shear viscosity is $\nu = 0.0035$, the vortex has initial radius $r_0 = 8.0$. After a number of iterations the vorticity of the flow is shown in Fig. 3. The rotational symmetry is obviously absent when the condition 35 is not satisfied, (right feature). The feature on the left uses only the second condition of Eq.35 as the first one is incompatible with numerical stability for small shear viscosity.

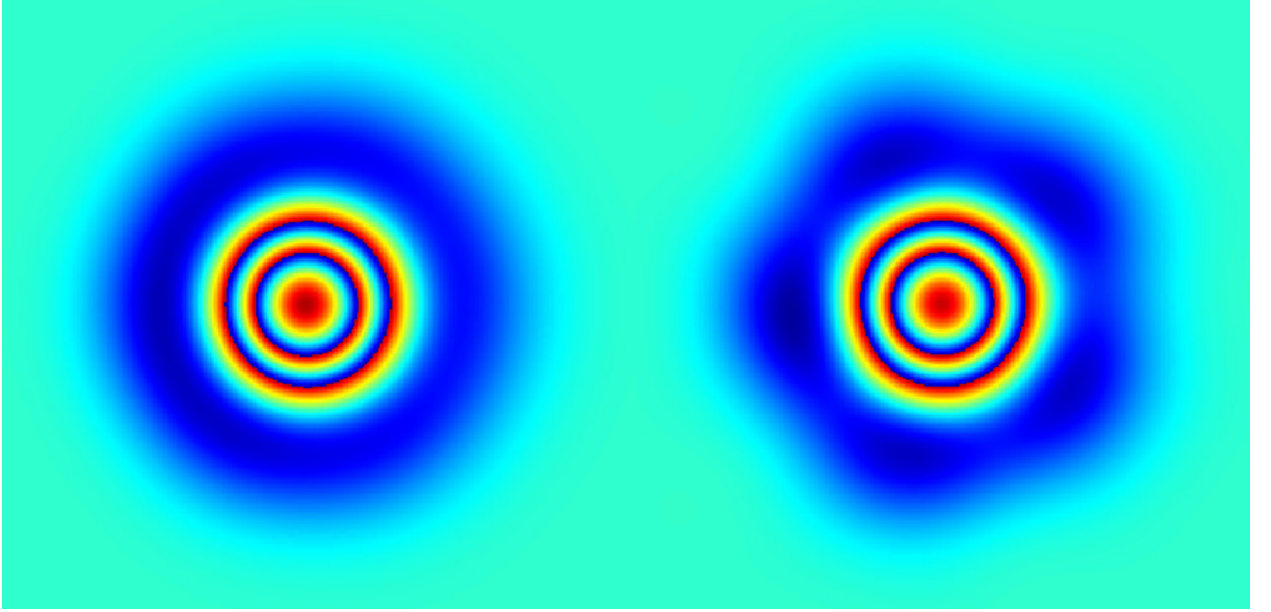


Figure 3: Simulation with D2Q9. Vorticity of the velocity field from an initial gaussian stream function after 9000 time steps for an advection velocity $\{0.03, 0.00\}$. Left with isotropy condition $12\sigma_4\sigma_6 = 1$. Right: arbitrary conditions.

Navier–Stokes D2Q13

In a first study, one considers the advection of shear plane waves by a uniform velocity V parallel to the wave vector. The domain is periodic of size 240×240 which corresponds to a smallest wave vector $k_0 = 2\pi/240$. Various cases are indicated below with numerical values of the relative advection either “experimental” as determined from simulations or theoretical using expressions given above.

Case	k_x/k_0	k_y/k_0	k/k_0	Simulation	Theory	Relative Error
A	5	12	13	0.9959	0.9960	0.01 %
B	10	24	26	0.9827	0.9840	0.13 %
C	13	0	13	0.9915	0.9917	0.02 %
D	26	0	26	0.9652	0.9666	0.15 %

Cases A and B, respectively C and D, correspond to the same orientation of the wave vector. The data clearly show an increase of the anomaly of the advection when the wave vector

increases and an effect of the orientation.

In a second study, simulation of the D2Q13 model have seen performed in a 363^2 domain with periodic boundary conditions. The initial condition is uniform speed (indicated in the caption), the shear viscosity is $\nu = 0.003$, the vortex has radius $r_0 = 11.0$. After a number of iterations the vorticity of the flow is shown in Fig. 4. The rotational symmetry is obviously absent. For comparison the figure also shows what is obtained without velocity.

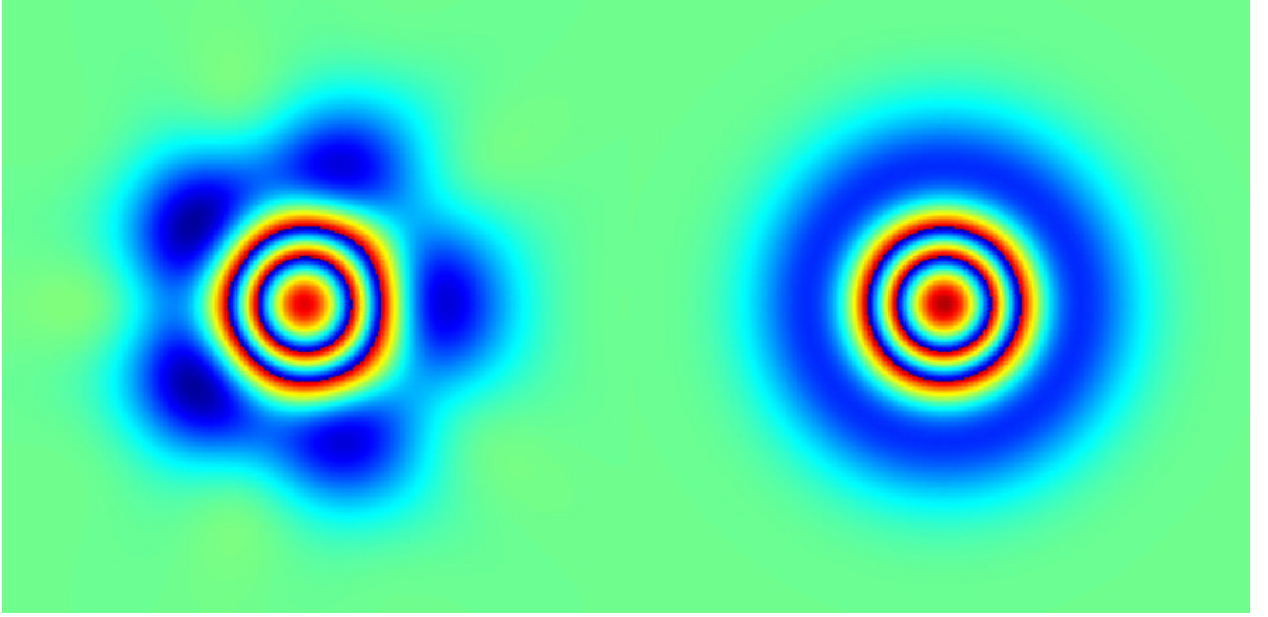


Figure 4: Simulation with D2Q13. Vorticity of the velocity field from an initial Gaussian stream function after 2770 time steps. Left with an advection velocity $\{0.10, 0.00\}$. Right with no advection.

Qualitative interpretation

To confirm qualitatively the influence of anomalous advection for the present case, the advection is treated in Fourier space. The initial stream function ψ can be represented as

$$(55) \quad \pi r_0^2 \sum_{k_x, k_y} \exp \left[-r_0^2 \frac{k_x^2 + k_y^2}{4} \right]$$

and each Fourier component evolves as

$$(56) \quad \exp \left[\left(-\nu (k_x^2 + k_y^2) + \imath g(k) V \right) t \right]$$

For $g(k)$ depending on k , the resulting stream function and the associated vorticity can be computed numerically. An example of such computations is shown in Fig. 5.

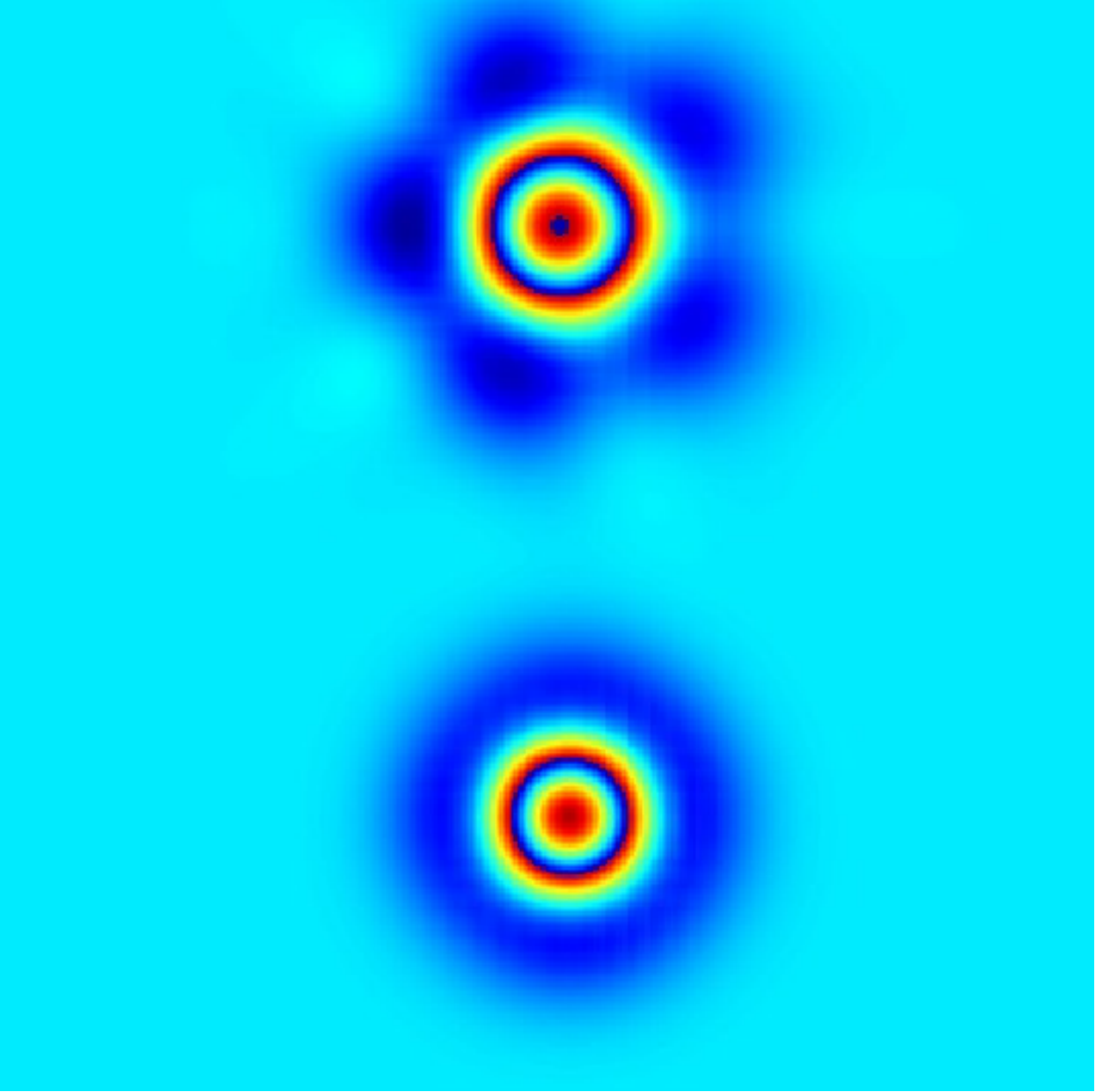


Figure 5: Vorticity of the vortex with main velocity at 14° from Ox and $r_0 = 4$ in a domain of size 80×80 . Initial state at bottom, final state at top. The advection used is $g(k) = 1 + 0.01 (\cos(4\theta) - \cos(2\theta)) k^2$.

The advection-diffusion case has also been studied in 3-D cases. As recalled earlier, the simple and popular D3Q7 is inadequate as the diffusivity depends on the square of the advective velocity, so we give results for D3Q15 and D3Q19 in Appendix 3.

Conclusion

It has been shown in the present report that lattice Boltzmann models can be tuned to reduce or in some cases eliminate defects that occur when they are used to simulate situations of flows with significant velocities or with features of rather small scales. However the analysis has been performed only in linearized situations, so that much work remains to be done for actual nonlinear flows in particular to estimate the errors due to inaccuracies in the advection which were pointed by Frisch for the early lattice gas models [11].

Appendix 1) Moments for the D2Q13 lattice Boltzmann scheme

For the D2Q13 model, we use the moments built with the polynomials given in Table 2. The equilibrium values are given in the following Table 5.

Moment	Parity	Rate	Equilibrium
ρ	+	0	ρ
j_x	−	0	j_x
j_y	−	0	j_y
E	+	s_3	$\alpha\rho + 13 \frac{j_x^2 + j_y^2}{\rho}$
XX	+	s_4	$\frac{j_x^2 - j_y^2}{\rho}$
XY	+	s_4	$\frac{j_x j_y}{\rho}$
Q_x	−	s_6	$j_x \left(c_1 - \frac{36q - 35}{77} (j_x^2 + j_y^2) \right)$
Q_y	−	s_6	$j_y \left(c_1 - \frac{36q - 35}{77} (j_x^2 + j_y^2) \right)$
R_x	−	s_8	$j_x \left(-\frac{63c_1 + 65}{24} + q j_x^2 + \frac{42q - 105}{22} j_y^2 \right)$
R_y	−	s_8	$j_y \left(-\frac{63c_1 + 65}{24} + \frac{42q - 105}{22} j_x^2 + q j_y^2 \right)$
E_2	+	s_{10}	$\beta \rho$
E_3	+	s_{11}	$\gamma \rho$
XYZ	−	s_{12}	0

Table 5: Moments of the D2Q13 lattice Boltzmann scheme for fluid flow including a tuning parameter q .

The relaxation phase uses the following relaxation rates and equilibrium value, such that the speed of sound waves in $c_s = \sqrt{(\alpha + 28)/26}$ and the shear and bulk viscosities are

$$(57) \quad \nu_0 = \frac{1}{4}(c_1 + 3)\sigma_4, \quad \zeta_0 = \frac{1}{26}(13c_1 - \alpha + 11)\sigma_3.$$

In the presence of a mean velocity, the shear viscosity is

$$(58) \quad \nu(V) = \nu_0 \left[1 - \frac{12(7 + 6q)}{77(3 + c_1)} V^2 \right]$$

leading to optimize the model with $q = -7/6$.

Appendix 2) Advection-diffusion for three-dimensional situations

D3Q15

The model follows the usual D3Q15 based of elementary velocities $\{0, 0, 0\}$, and permutations of $\{1, 1, 1\}$ and of $\{1, 0, 0\}$. The moments are computed with the matrix

$$(59) \quad M = \begin{pmatrix} 1 & 1 & 1 & 1 & 1 & 1 & 1 & 1 & 1 & 1 & 1 & 1 & 1 & 1 & 1 \\ 0 & 1 & -1 & 0 & 0 & 0 & 0 & 1 & -1 & 1 & -1 & 1 & -1 & 1 & -1 \\ 0 & 0 & 0 & 1 & -1 & 0 & 0 & 1 & 1 & -1 & -1 & 1 & 1 & -1 & -1 \\ 0 & 0 & 0 & 0 & 0 & 1 & -1 & 1 & 1 & 1 & 1 & -1 & -1 & -1 & -1 \\ -2 & -1 & -1 & -1 & -1 & -1 & -1 & 1 & 1 & 1 & 1 & 1 & 1 & 1 & 1 \\ 0 & 2 & 2 & -1 & -1 & -1 & -1 & 0 & 0 & 0 & 0 & 0 & 0 & 0 & 0 \\ 0 & 0 & 0 & 1 & 1 & -1 & -1 & 0 & 0 & 0 & 0 & 0 & 0 & 0 & 0 \\ 0 & 0 & 0 & 0 & 0 & 0 & 0 & 1 & -1 & -1 & 1 & 1 & -1 & -1 & 1 \\ 0 & 0 & 0 & 0 & 0 & 0 & 0 & 1 & 1 & -1 & -1 & -1 & -1 & 1 & 1 \\ 0 & 0 & 0 & 0 & 0 & 0 & 0 & 1 & -1 & 1 & -1 & -1 & 1 & -1 & 1 \\ 0 & -4 & 4 & 0 & 0 & 0 & 0 & 1 & -1 & 1 & -1 & 1 & -1 & 1 & -1 \\ 0 & 0 & 0 & -4 & 4 & 0 & 0 & 1 & 1 & -1 & -1 & 1 & 1 & -1 & -1 \\ 0 & 0 & 0 & 0 & 0 & -4 & 4 & 1 & 1 & 1 & 1 & -1 & -1 & -1 & -1 \\ 16 & -4 & -4 & -4 & -4 & -4 & -4 & 1 & 1 & 1 & 1 & 1 & 1 & 1 & 1 \\ 0 & 0 & 0 & 0 & 0 & 0 & 0 & 1 & -1 & -1 & 1 & -1 & 1 & 1 & -1 \end{pmatrix}.$$

associated to the orthogonal polynomials :

Parity	
+	1
−	x
−	y
−	z
+	$-2 + x^2 + y^2 + z^2$
+	$2 x^2 - y^2 - z^2$
+	$y^2 - z^2$
+	$x y$
+	$y z$
+	$z x$
−	$x (-13/2 + 5/2 (x^2 + y^2 + z^2))$
−	$y (-13/2 + 5/2 (x^2 + y^2 + z^2))$
−	$z (-13/2 + 5/2 (x^2 + y^2 + z^2))$
+	$16 - 55/2 (x^2 + y^2 + z^2) + 15/2 (x^2 + y^2 + z^2)^2$
−	$x y z$

In the presence of a uniform advective velocity $\{V_x, V_y, V_z\}$, the relaxation rates s_i and the equilibrium values of the non-conserved moments are given by the following Table.

Moment	Parity	Rate	Equilibrium
ρ	+	0	0
\dot{j}_x	−	s_1	ρV_x
\dot{j}_y	−	s_1	ρV_y
\dot{j}_z	−	s_1	ρV_z
ee	+	s_5	$\alpha \rho + \rho (V_x^2 + V_y^2 + V_z^2)$
xx	+	s_6	$\rho (2 V_x^2 - V_y^2 - V_z^2)$
yy	+	s_6	$\rho (V_y^2 - V_x^2 - V_z^2)$
xy	+	s_6	$\rho V_x V_y$
yz	+	s_6	$\rho V_y V_z$
zx	+	s_6	$\rho V_z V_x$
q_x	−	s_{11}	$d_1 \rho V_x$
q_y	−	s_{11}	$d_1 \rho V_y$
q_z	−	s_{11}	$d_1 \rho V_z$
$d3$	+	s_{14}	$\beta \rho$
tt	−	s_{15}	0

Table 6: Equilibrium moments for advective D3Q15.

This leads to an effective diffusivity

$$(60) \quad \kappa = \frac{2 + \alpha}{3} \sigma_1$$

independent of the velocity. The analysis of the anomalous advection shows that it can be suppressed for two conditions.

First case

$$(61) \quad \sigma_5 = \frac{4}{(1 + 3\alpha)} \sigma_6 - \frac{6(2 + \alpha)}{(1 + 3\alpha)} \sigma_1 + \frac{3(1 + \alpha)}{4(1 + 3\alpha)} \frac{1}{\sigma_1} \quad \text{for } d_1 = -\frac{7}{3}.$$

Second case

$$(62) \quad \sigma_5 = \frac{10(2 + \alpha)}{(3 + 2d_1 - 5\alpha)} \sigma_1 - \frac{15\alpha - 2d_1 + 17}{12(3 + 2d_1 - 5\alpha)} \frac{1}{\sigma_1} \quad \text{for } \sigma_6 = \frac{1}{12\sigma_1}.$$

D3Q19

The model follows the usual D3Q19 based of elementary velocities $\{0, 0, 0\}$, and permutations

of $\{1, 1, 0\}$ and of $\{1, 0, 0\}$. The moments are computed with the following matrix M :

$$(63) \quad \begin{pmatrix} 1 & 1 & 1 & 1 & 1 & 1 & 1 & 1 & 1 & 1 & 1 & 1 & 1 & 1 & 1 & 1 & 1 \\ 0 & 1 & -1 & 0 & 0 & 0 & 0 & 1 & -1 & 1 & -1 & 0 & 0 & 0 & 1 & 1 & -1 & -1 \\ 0 & 0 & 0 & 1 & -1 & 0 & 0 & 1 & 1 & -1 & -1 & 1 & -1 & 1 & -1 & 0 & 0 & 0 \\ 0 & 0 & 0 & 0 & 0 & 1 & -1 & 0 & 0 & 0 & 0 & 1 & 1 & -1 & -1 & 1 & -1 & -1 \\ -30 & -11 & -11 & -11 & -11 & -11 & -11 & 8 & 8 & 8 & 8 & 8 & 8 & 8 & 8 & 8 & 8 & 8 \\ 0 & 2 & 2 & -1 & -1 & -1 & -1 & 1 & 1 & 1 & 1 & -2 & -2 & -2 & -2 & 1 & 1 & 1 \\ 0 & 0 & 0 & 1 & 1 & -1 & -1 & 1 & 1 & 1 & 1 & 0 & 0 & 0 & 0 & -1 & -1 & -1 \\ 0 & 0 & 0 & 0 & 0 & 0 & 0 & 1 & -1 & -1 & 1 & 0 & 0 & 0 & 0 & 0 & 0 & 0 \\ 0 & 0 & 0 & 0 & 0 & 0 & 0 & 0 & 0 & 0 & 0 & 1 & -1 & -1 & 1 & 0 & 0 & 0 \\ 0 & 0 & 0 & 0 & 0 & 0 & 0 & 0 & 0 & 0 & 0 & 0 & 0 & 0 & 0 & 1 & -1 & -1 \\ 0 & -4 & 4 & 0 & 0 & 0 & 0 & 1 & -1 & 1 & -1 & 0 & 0 & 0 & 0 & 1 & 1 & -1 \\ 0 & 0 & 0 & -4 & 4 & 0 & 0 & 1 & 1 & -1 & -1 & 1 & -1 & 1 & -1 & 0 & 0 & 0 \\ 0 & 0 & 0 & 0 & 0 & -4 & 4 & 0 & 0 & 0 & 0 & 1 & 1 & -1 & -1 & 1 & -1 & -1 \\ 0 & -4 & -4 & 2 & 2 & 2 & 2 & 1 & 1 & 1 & 1 & -2 & -2 & -2 & -2 & 1 & 1 & 1 \\ 0 & 0 & 0 & -2 & -2 & 2 & 2 & 1 & 1 & 1 & 1 & 0 & 0 & 0 & 0 & -1 & -1 & -1 \\ 12 & -4 & -4 & -4 & -4 & -4 & -4 & 1 & 1 & 1 & 1 & 1 & 1 & 1 & 1 & 1 & 1 & 1 \\ 0 & 0 & 0 & 0 & 0 & 0 & 0 & 1 & -1 & 1 & -1 & 0 & 0 & 0 & 0 & -1 & -1 & 1 \\ 0 & 0 & 0 & 0 & 0 & 0 & 0 & -1 & -1 & 1 & 1 & 1 & -1 & 1 & -1 & 0 & 0 & 0 \\ 0 & 0 & 0 & 0 & 0 & 0 & 0 & 0 & 0 & 0 & 0 & -1 & -1 & 1 & 1 & 1 & -1 & -1 \end{pmatrix}.$$

associated to the orthogonal polynomials :

Parity	
+	1
−	x
−	y
−	z
+	$-30 + 19 (x^2 + y^2 + z^2)$
+	$2 x^2 - y^2 - z^2$
+	$y^2 - z^2$
+	$x y$
+	$y z$
+	$z x$
−	$x (-9 + 5 (x^2 + y^2 + z^2))$
−	$y (-9 + 5 (x^2 + y^2 + z^2))$
−	$z (-9 + 5 (x^2 + y^2 + z^2))$
+	$(2 x^2 - y^2 - z^2) (-5 + 3 (x^2 + y^2 + z^2))$
+	$(y^2 - z^2) (-5 + 3 (x^2 + y^2 + z^2))$
+	$12 - 53/2 (x^2 + y^2 + z^2 + 21/2 (x^2 + y^2 + z^2)^2)$
−	$x (y^2 - z^2)$
−	$y (z^2 - x^2)$
−	$z (x^2 - y^2)$

In the presence of a uniform advective velocity $\{V_x, V_y, V_z\}$, the relaxation rates s_i and the equilibrium values of the non-conserved moments are given by the Table 7.

Applying the same analysis as for D2Q9, one can show that the effective diffusivity is

$$(64) \quad \kappa = \frac{\alpha + 30}{57} \left(\frac{1}{s_1} - \frac{1}{2} \right)$$

Moment	Parity	Rate	Equilibrium
ρ	+	0	ρ
j_x	−	s_1	$V_x \rho$
j_y	−	s_1	$V_y \rho$
j_z	−	s_1	$V_z \rho$
ee	+	s_5	$\alpha \rho + 19 (V_x^2 + V_y^2 + V_z^2) \rho$
xx	+	s_6	$(2 V_x^2 - V_y^2 - V_z^2) \rho$
yy	+	s_6	$(V_y^2 - V_x^2) \rho$
xy	+	s_6	$V_x V_y \rho$
yz	+	s_6	$V_y V_z \rho$
zx	+	s_6	$V_z V_x \rho$
q_x	−	s_{11}	$d_1 V_x \rho$
q_y	−	s_{11}	$d_1 V_y \rho$
q_z	−	s_{11}	$d_1 V_z \rho$
xxe	+	s_{14}	0
yye	+	s_{14}	0
$d3$	+	s_{16}	$\beta \rho$
t_x	−	s_{17}	$d_2 V_x \rho$
t_y	−	s_{17}	$d_2 V_y \rho$
t_z	−	s_{17}	$d_2 V_z \rho$

Table 7: Equilibrium moments for the diffusive D3Q19 lattice Boltzmann scheme

independent of the velocity V . The order 3 for the equivalent equation includes terms linear in applied velocity that can be interpreted as corrections to the advection factor. This correction can be suppressed with two possible sets of parameters.

First case

For $d_1 = -2/3$ and $d_2 = 0$, the relaxation rate s_5 should satisfy:

$$(65) \quad \sigma_5 = \frac{76}{3\alpha - 5} \sigma_6 + \frac{6(\alpha + 30)}{5 - 3\alpha} \sigma_1 + \frac{3(11 + \alpha)}{4(3\alpha - 5)} \frac{1}{\sigma_1}$$

where $\sigma_i = \frac{1}{s_i} - \frac{1}{2}$ is the Hénon parameter.

Second case

For $\sigma_6 = \frac{1}{12\sigma_1}$, the relaxation rate s_5 should satisfy:

$$(66) \quad \sigma_5 = \frac{10(\alpha + 30)}{21 + 19d_1 - 5\alpha} \sigma_1 - \frac{279 - 19d_1 + 15\alpha}{12(21 + 19d_1 - 5\alpha)} \frac{1}{\sigma_1}$$

Values of the parameters will be constrained by stability conditions, in particular $\sigma_5 > 0$.

Two Relaxation Times (TRT)

Note that most of the relaxation rates do not appear in the previous conditions, so one can use the simpler TRT situation (with only two relaxation rates, one for + parity and one for − parity). The various results shown in this Appendix are summarized in the table 8 that applies to the TRT case.

Case	Conditions
D3Q19-1	$d_1 = -\frac{2}{3}, \quad d_2 = 0, \quad \sigma_6 = \frac{2(30 + \alpha)}{27 - \alpha} \sigma_1 - \frac{11 + \alpha}{27 - \alpha} \frac{1}{4 \sigma_1}$
D3Q19-2	$\sigma_1 = \frac{1}{\sqrt{12}}, \quad \sigma_6 = \frac{1}{\sqrt{12}}$
D3Q15-1	$d_1 = -\frac{7}{3}, \quad \sigma_6 = 2 \frac{2 + \alpha}{1 - \alpha} \sigma_1 - \frac{1 + \alpha}{1 - \alpha} \frac{1}{4 \sigma_1}$
D3Q15-2	$\sigma_1 = \frac{1}{\sqrt{12}}, \quad \sigma_6 = \frac{1}{\sqrt{12}}$

Table 8: Isotropy of anomalous advection : results for the TRT situation.

To be complete, we add some results for the “hyper-diffusivity” derived from the equivalent equations at order 4.

Appendix 3)

Hyper-diffusivity of the three-dimensional diffusion models

In the absence of an advection velocity, one can easily obtain the “hyper-diffusivity” carrying out the equivalent process to fourth order. The formula are quite complicated so we only give conditions for obtaining a null hyper-diffusivity like was done for the shear hyper-viscosity.

D3Q15

$$(67) \quad \sigma_{11} = \frac{(8\alpha + \beta) + 14(\alpha + 2)(1 - 6\sigma_2\sigma_6)}{(8\alpha + \beta)(12\sigma_1\sigma_6 - 1)} \sigma_1,$$

$$(68) \quad \sigma_5 = \frac{\sigma_1}{4[5(\alpha + 2)(3\alpha + 1)(1 - 12\sigma_1\sigma_6) + 30(\alpha + 1) + 2(\beta - 1)]} \times \\ \{60(\alpha + 2)^2(12\sigma_1\sigma_6 - 1)\sigma_1^2 - 960(\alpha + 2)\sigma_1^2\sigma_6^2 \\ + 4(2\beta - 40\alpha + 68 - 45\alpha^2)\sigma_1\sigma_6 + 15(\alpha + 2)\alpha\}$$

D3Q19

$$(69) \quad \sigma_{11} = -\frac{1}{19} \sigma_1 \frac{84(\alpha + 30)\sigma_1\sigma_6 - 95\beta - 52\alpha - 420}{(2\alpha + 5\beta)(12\sigma_1\sigma_6 - 1)}$$

$$\begin{aligned}
 \sigma_5 = & - \frac{1}{4 \{ 84 (\alpha + 30)(3\alpha - 5)\sigma_1\sigma_6 - 21\alpha^2 - 722\beta - 937\alpha - 546 \} \sigma_1} \times \\
 (70) \quad & (1008 (\alpha + 30)^2 \sigma_1^3 \sigma_6 - 84((\alpha + 30)^2 + 304(\alpha + 30)\sigma_6^2)\sigma_1^2 \\
 & + 4(32676 - 63\alpha^2 - 512\alpha + 722\beta)\sigma_6\sigma_1 + 21(\alpha + 30)(\alpha - 8))
 \end{aligned}$$

These expressions can be simplified for the TRT case. One obtains the same results for the two models:

$$(71) \quad \sigma_1 = \sigma_{11} = \frac{1}{\sqrt{12}}, \quad \sigma_5 = \sigma_6 = \frac{1}{\sqrt{3}},$$

Note that one gets the same value of σ_1 as in Table 1, but a different one for σ_6 . It is thus not possible to have at the same time no anomalous convection and no hyper-diffusivity.

References

- [1] A. Augier, F. Dubois, B. Graille and P. Lallemand. “On rotational invariance of Lattice Boltzmann schemes”, *Computers and Mathematics with Applications*, vol. **67**, p 239-255, 2014.
- [2] F. Dubois. “Equivalent partial differential equations of a Boltzmann scheme”, *Computers and mathematics with applications*, vol. **55**, p. 1441-1449, 2008.
- [3] F. Dubois, “Nonlinear fourth order Taylor expansion of lattice Boltzmann schemes”, *Asymptotic Analysis*, vol. **127**, p. 297-337, 2022.
- [4] F. Dubois, P. Lallemand. “Towards higher order lattice Boltzmann schemes”, *Journal of Statistical Mechanics: Theory and Experiment*, P06006 doi: 10.1088/1742-5468/2009/06/P06006, 2009.
- [5] F. Dubois, P. Lallemand. “On Triangular Lattice Boltzmann Schemes for Scalar Problems”, *Communications in Computational Physics*, vol. **13**, p. 649-670, 2013.
- [6] M. H  non. “Viscosity of a Lattice Gas”, *Complex Systems*, vol. **1**, p. 763-789, 1987.
- [7] D. d’Humi  res. “Generalized Lattice-Boltzmann Equations”, in *Rarefied Gas Dynamics: Theory and Simulations*, vol. **159** of *AIAA Progress in Astronautics and Astronautics*, p. 450-458, 1992.
- [8] M. Junk, A. Klar, L.S. Luo. “Asymptotic analysis of the lattice Boltzmann equation”, *Journal of Computational Physics*, vol. **210**, p. 676-704, 2005.
- [9] P. Lallemand, L-S. Luo. “Theory of the lattice Boltzmann method: Dispersion, dissipation, isotropy, Galilean invariance, and stability”, *Physical Review E*, vol. **61**, p. 6546-6562, June 2000.
- [10] L.D. Landau, E.M. Lifshitz. *Fluid Mechanics* (Volume 6 of A Course of Theoretical Physics), Pergamon Press, 1959.
- [11] U. Frisch, private communication (May 1985).